AIP | The Journal of Chemical Physics

Collision cross section calculations for polyatomic ions considering rotating diatomic/linear gas molecules

Carlos Larriba-Andaluz and Christopher J. Hogan Jr.

Citation: The Journal of Chemical Physics **141**, 194107 (2014); doi: 10.1063/1.4901890
View online: http://dx.doi.org/10.1063/1.4901890
View Table of Contents: http://scitation.aip.org/content/aip/journal/jcp/141/19?ver=pdfcov
Published by the AIP Publishing

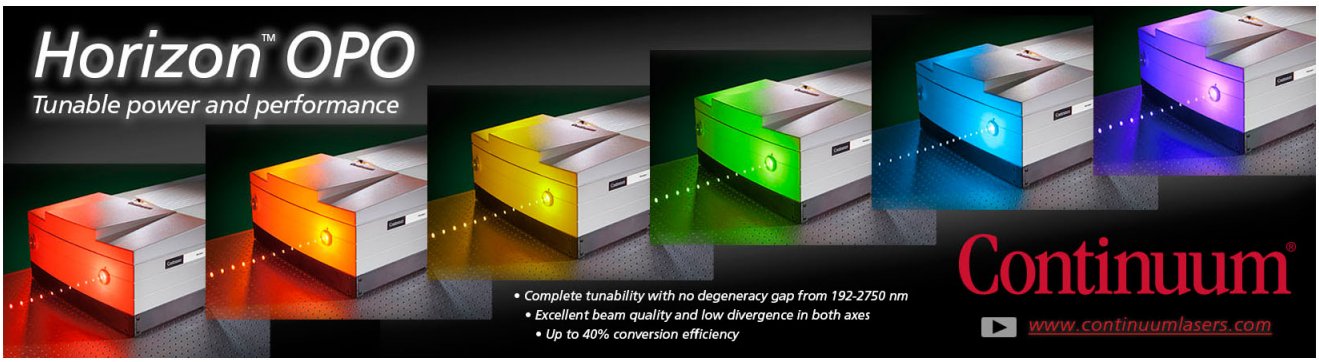

Collision cross section calculations for polyatomic ions considering rotating diatomic/linear gas molecules

Carlos Larriba-Andaluz[a] and Christopher J. Hogan, Jr.
Department of Mechanical Engineering, University of Minnesota, 111 Church St. S.E., Minneapolis, Minnesota 55455, USA

(Received 21 August 2014; accepted 3 November 2014; published online 18 November 2014)

Structural characterization of ions in the gas phase is facilitated by measurement of ion collision cross sections (CCS) using techniques such as ion mobility spectrometry. Further information is gained from CCS measurement when comparison is made between measurements and accurately predicted CCSs for model ion structures and the gas in which measurements are made. While diatomic gases, namely molecular nitrogen and air, are being used in CCS measurement with increasingly prevalency, the majority of studies in which measurements are compared to predictions use models in which gas molecules are spherical or non-rotating, which is not necessarily appropriate for diatomic gases. Here, we adapt a momentum transfer based CCS calculation approach to consider rotating, diatomic gas molecule collisions with polyatomic ions, and compare CCS predictions with a diatomic gas molecule to those made with a spherical gas molecular for model spherical ions, tetra-alkylammonium ions, and multiply charged polyethylene glycol ions. CCS calculations are performed using both specular-elastic and diffuse-inelastic collisions rules, which mimic negligible internal energy exchange and complete thermal accommodation, respectively, between gas molecule and ion. The influence of the long range ion-induced dipole potential on calculations is also examined with both gas molecule models. In large part we find that CCSs calculated with specular-elastic collision rules decrease, while they increase with diffuse-inelastic collision rules when using diatomic gas molecules. Results clearly show the structural model of both the ion and gas molecule, the potential energy field between ion and gas molecule, and finally the modeled degree of kinetic energy exchange between ion and gas molecule internal energy are coupled to one another in CCS calculations, and must be considered carefully to obtain results which agree with measurements.
 [http://dx.doi.org/10.1063/1.4901890]

INTRODUCTION

Ion mobility spectrometry[1,2] (IMS) enables the separation and structural characterization of gas phase ions. In the free molecular regime, at low ion velocity to mean thermal speed ratios (conditions applicable in most IMS systems), the ion mobility, Z_p, can be calculated as[3]

$$Z_p = \sqrt{\frac{\pi}{8 m_{red} k T}} \frac{3}{4 n_{gas}} \frac{z e}{\Omega}, \tag{1}$$

where m_{red} is the reduced mass for the gas molecule/ion pair, k is Boltzmann's constant, T is the temperature, z is the net number of integer (positive or negative) charges on the ion, e is the unit charge, n_{gas} is the gas molecule number concentration, and Ω is the ion's collision cross section (CCS). The CCS is a complex parameter, dependent upon the potential interactions between gas molecules and the ion, the gas molecule and ion structures, and the degree of thermal energy exchange in the ion and gas molecule upon collision.[4] The subject of debate in numerous studies,[5–13] it is essential to find an accurate method for calculation of CCSs, as other than the ion charge state, it is the CCS which uniquely defines ion mobility for different ions in a given bath gas, and thus facilitates IMS separation.

Previously developed methods[8–11,14–17] for CCS calculation differ from one another primarily on the presumed manner in which impinging gas molecules are reemitted upon collision with the ion, which, outside of the large ion limit (i.e., below ∼ 10 nm in ion size) lead to significantly different CCSs. Seminal IMS studies using helium as a drift gas considered specular-elastic hard sphere scattering (EHSS) for gas molecule reemission, and show that in this gas such a reemission law can lead to good agreement between measured and calculated CCSs for ions with reasonably unambiguous structures.[18–21] However, purely specular scattering of assumed spherical gas molecules from rigid ion surfaces, in which the gas molecule translational kinetic energy is conversed before and after collision, does not appear to explain many experimental observations in diatomic gases, i.e., diatomic nitrogen[12,22] and air.[23,24] On the contrary, the manner in which gas molecules impinge upon and are remitted from polyatomic ions which, in reality, are entities with their own rotational, vibrational, and translational degrees of freedom, is strongly drift gas dependent,[4] i.e., exchange between different modes of thermal energy in gas molecules and ions occurs during collisions,[25–27] and without modeling all modes of energy, gas-specific,

[a]Author to whom correspondence should be addressed. Electronic mail: clarriba@umn.edu

"coarse-grained" collision rules need to be developed to model this exchange.

Recently, invoking the arguments of Millikan[28] and Epstein,[29] we have suggested[8,9] that when considering spherical gas molecules and rigid ions in calculations but attempting to predict CCSs in non-monoatomic/heavier gases, it is more appropriate to invoke a gas molecule reemission rule in which both the angle of reemission and the gas molecule reemission speed are selected randomly from pre-defined distributions based upon the ion's temperature (i.e., gas molecule reemission is effectively diffuse, with significant exchange between translational, rotational, and vibrational energy during collisions). The invoked gas molecule reemission rules lead to good agreement between CCS calculations and measurements for multiply charged polymer ions and singly charged tetraalkylammonium ions in air. These rules are, unfortunately, strictly empirical, and in a recent comparison[5] of CCS measurements of alkali metal iodide salt cluster ions in air to predictions, we found that neither specular EHSS, nor diffuse, inelastic reemission rule CCS predictions agree with all measurements.

The ultimate goal in CCS calculation is to develop an approach which accurately considers ion-gas molecule potential interactions (potential energy changes), as well as both ion and gas molecule rotation and vibration (kinetic energy changes)[30] during collisions. Regrettably, development of a calculation routine modeling potential and kinetic energy exactly is not only theoretically cumbersome, but also the computational cost is presently prohibitive for an appreciably large polyatomic ion. For this reason, we aim to produce a set of algorithms that mimic gas molecule-ion collision dynamics in an efficient and thermodynamically permissible manner, and along these lines we have developed IMoS (Ion Mobility Software, available directly from the corresponding author), which is series of methods[8] to calculate CCSs of polyatomic ion models through momentum transfer calculations. A variety of empirical gas molecule impingement-reemission rules can be invoked in these methods and the influence of long range potentials (as well as Lennard-Jones potentials) between gas molecules and polyatomic ions can be considered. However, to date the gas molecule has been considered spherical in all IMoS calculations. In the present report, we adapt the IMoS algorithms to consider a diatomic molecule and describe its rotation through a Maxwell angular velocity distribution. Collisions are modeled via rigid body dynamics between a doublet and a rigid ion structure, taking special care to allow for conservation of energy with prescribed impingement and reemission rules (either elastic and specular or inelastic and diffuse). While diatomic gas molecules have been modeled in prior studies,[12,22] only specular-elastic collisions have been considered, and the computational cost involved in CCS prediction with these models prohibits calculations for ions composed of more than ~20 atoms within a reasonable time frame, with modest computational power. The approach presented here enables CCS calculations for polyatomic ions composed of 2000 atoms or larger to be computed within a few hours on a standard laptop or desktop computer with accuracies in CCSs within 1%. Calculation results are reported considering molecular nitrogen as the bath gas for spherical ions (and compared to analytical solutions for collisions with monoatomic gas molecules), tetraalkylammonium ions,[31] and polyethylene glycol ions.[32] Comparison to experimental data measured near room temperature is provided for the polyatomic ions. While we show how calculations with rigid diatomic gas molecules can be performed, the present study does not elucidate the proper impingement-reemission rules to employ in CCS calculations under all conditions (i.e., with different drift gases and at different temperatures); rather it shows that even with gas molecule rotation considered, specular-elastic collision rules do not lead to calculated CCSs in line with measurements in diatomic gases. Further, calculation results show that in addition to the collision rules applied, the physical model of gas molecules (as spheres, diatoms, etc.) influences CCS calculations, with the gas molecule structure and collision rules chosen coupled to one another.

CALCULATION METHODS

The free molecular momentum transfer algorithms invoked are described in detail in prior reports[8,9] and have been incorporated into the ion mobility calculation scheme IMoS (available freely from the corresponding author; an image of the IMoS GUI is available in the supplementary material).[35] To modify these algorithms to calculate collision cross sections considering diatomic molecules in lieu of monoatomic molecules, it is necessary to (1) alter the structural description of the gas molecules, (2) correctly sample the gas molecule initial conditions, and (3) correctly model gas molecule impingement and reemission, accounting for exchange between translational and vibrational energy upon collision. Items (1) and (2) are described in the subsequent *Diatomic Gas Molecule Structure and Rotational Velocity Distribution* section, while item (3) is described in the *Gas Molecule Impingement and Reemission* section. In adapting IMoS algorithms to consider the structure and rotation of diatomic/linear gas molecules, we apply hard sphere scattering algorithms, in which all atoms are defined by their radii and gas molecule reemission and impingement is either diffuse or specular (i.e., with a random selected remission angle or a predetermined angle) as well as either elastic or inelastic, i.e., with no energy exchange with unmodeled degrees of freedom (elastic), or with complete thermal accommodation in all degrees of freedom upon collision (inelastic). We additionally consider the influence of the ion-induced dipole potential on gas molecule trajectories, using the simplified velocity distribution algorithm from Larriba and Hogan.[8] In accounting for the induced dipole potential, we do not constrain the rotation of the gas molecule; a freely rotating gas molecule is an assumption in all presented calculations.

Diatomic gas molecule structure and rotational velocity distribution

As depicted in Figure 1, each diatomic gas molecule is treated as a pair of heavy masses rigidly joined together (a rigid doublet), i.e., no vibrational energy is considered. To set the bond distance and moment of inertia of the doublet, in the

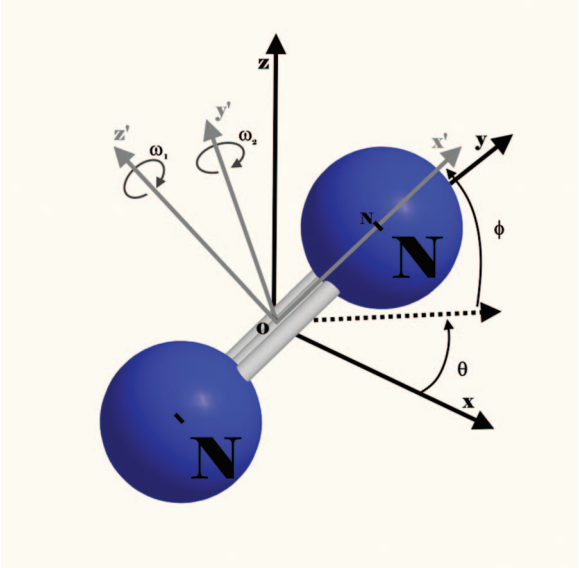

FIG. 1. Schematic of the diatomic molecule position (using θ,ϕ) and angular velocity in space (w_1,w_2). The molecule is composed of two heavy masses each a distance r_{ON} from the center.

present study we model N_2 using the parameters from Niwa *et al.*,[33] with which the diatomic molecule has an interatomic distance, $r_{N\text{-}N}$, of 0.98 Å and a radius, r_N, of 1.335 Å for each of the atoms. The gas molecule's moment of inertia perpendicular to the connecting axis of the diatomic molecule at the center of mass, I_1, is given by

$$I_1 = m_{gas}\left(\frac{r_{N-N}}{2}\right)^2, \tag{2}$$

where m_{gas} is the N_2 molecule mass. For comparison to prior approaches, the sphere-equivalent radius from the average projected area of the noted diatomic molecule is approximately 1.55 A, in accordance with previous measurements of nitrogen and "air" molecules.[23,24]

In IMoS calculations, CCSs are determined by examining the rate of momentum transfer (i.e., the drag force) from gas molecules to an ion, represented by a fixed structural model, in the presence of a small translational ion velocity.[8] Gas molecules are introduced into the system through the surface of a control volume (either rectangular or cuboid) circumscribing the ion; gas molecule initial coordinates are sampled appropriately for the ion velocity considered and each gas molecule's initial velocity vector is determined by sampling its speed and entry angles from appropriate distributions.[8] In addition to this, for a diatomic gas molecule, an initial orientation and rotational velocity vector must be prescribed. With the gas molecule's relative speed (to the ion) and the position of its center defined as the origin in a directionally fixed spherical coordinate system with coordinates r, θ, and ϕ (labelled in Figure 1), the rotational energy, E_R, is defined as[34]

$$E_R = \frac{1}{2}m_{gas}\left(\frac{r_{N-N}}{2}\right)^2(\dot\theta^2 + \sin^2\theta\dot\phi^2) = \frac{I_1}{2}(\dot\theta^2 + \sin^2\theta\dot\phi^2), \tag{3a}$$

where the term in parenthesis in Eq. (3a) corresponds to the two components of the angular velocity. We note the rotational energy can also be expressed as

$$E_R = \frac{I_1}{2}\left(w_1^2 + w_2^2\right) = \frac{1}{2}I_1 w^2, \tag{3b}$$

where w is the magnitude of the angular velocity, $w_1 = \dot\theta$ and $w_2 = \sin\theta\dot\phi$. Assuming thermal equilibrium outside the boundaries of the control volume, the probability of a gas molecule having its angular velocity in the elementary region $dw_1 dw_2$ (i.e., the probability distribution function) is given by

$$\begin{aligned} P(\theta,\phi,w_1,w_2) &= Ke^{-\frac{E_R}{kT}}\sin\theta d\theta d\phi dw_1 dw_2 \\ &= Ke^{-\frac{I_1}{2kT}\left(w_1^2+w_2^2\right)}\sin\theta d\theta d\phi dw_1 dw_2, \end{aligned} \tag{4}$$

where K is a partition function that allows the cumulative probability to converge to 1 when integrated over all spatial variables. When applying this distribution, the orientation and angular velocity of the molecule when entering the control volume is completely random and can be given by a suitable set of random angles (θ,ϕ) and velocities (w_1,w_2). By making a suitable change of angular velocity variables:

$$w = \sqrt{w_1^2 + w_2^2}, \tag{5a}$$

$$\tan\psi = \frac{w_1}{w_2}, \tag{5b}$$

all variables in Eq. (4) can be made separable:

$$P(\theta,\phi,d\psi,w) = Ke^{-\frac{I_1}{2kT}(w^2)}w\sin\theta d\theta d\phi d\psi dw, \tag{5c}$$

and hence each variable can be sampled from the following equations:

$$\phi = 2\pi R_1, \tag{6a}$$

$$\cos\theta = 1 - 2R_2, \tag{6b}$$

$$\psi = 2\pi R_3, \tag{6c}$$

$$w = \sqrt{\frac{2kT}{I_1\ln(1-R_4)}}, \tag{6d}$$

where R_1, R_2, R_3, and R_4 are uniformly distributed variables on the interval 0 to 1. Equations (6a)–(6d) hence enable determination of each gas molecule's initial orientation and rotational velocity. Finally, the inertia tensor for a diatomic gas molecule is given as

$$I = \begin{bmatrix} 0/\infty & 0 & 0 \\ 0 & I_1 & 0 \\ 0 & 0 & I_1 \end{bmatrix}. \tag{7}$$

After sampling each gas molecule's initial orientation and rotational velocity, this tensor is rotated to match the initial condition using appropriate rotation matrices, as is demonstrated in the supplementary material.[35]

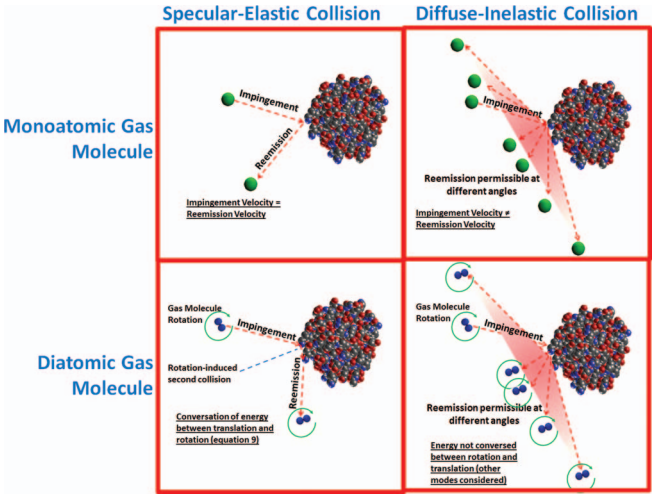

FIG. 2. Depiction of impingement and reemission for monoatomic and diatomic gas molecules based on both specular-elastic and diffuse-inelastic collision rules with a rigid ion structure. The ion model is based on the crystal structure of cytochrome C.

Gas molecule impingement and reemission

On entering the control volume, a gas molecule will travel with a constant angular velocity until it either exits the domain or impinges upon (collides with) the ion. After impingement, a set of reemission rules is invoked wherein linear and angular momentum are conserved, but translational and rotational energy exchange is permissible. Reemission possibilities for both monoatomic and diatomic gas molecules are depicted in Figure 2. When a gas molecule-ion collision occurs, a bisection method is used to determine the exact time and point of collision with large precision (with an error in position of less than 0.5% of the diameter of gas molecule), hence the particular atoms colliding are readily identified. Rigid body mechanics must be invoked to subsequently describe gas molecule reemission, and the set of rules applied must be modified depending on whether the gas molecule reemission is modeled as specular and elastic (in which the exchange of energy with non-modeled degrees of internal energy in the ion and gas molecules is neglected), or diffuse and inelastic (complete equilibration of all degrees of thermal energy are assumed at the temperature of the ion).

In the case of specular and elastic reemission, following rigid body equations for the collision between a fixed object and a moving rigid body at a given location $\vec{a}$, the reemitted translational velocity, $\vec{v}_r$, and reemitted angular velocity, $\vec{w}_r$ are given by the equations:[36,37]

$$\vec{v}_r = \vec{v}_c + \frac{j\vec{n}_a}{m_{gas}}, \tag{8a}$$

$$\vec{w}_r = \vec{w} + I^{-1}(\vec{r} \times j\vec{n}_a), \tag{8b}$$

where j is the impulse, given by

$$j = \frac{2(\vec{v}_c + \vec{w} \times \vec{r}_a) \cdot \vec{n}_a}{\frac{1}{m_{gas}} + \vec{n}_a \cdot (I^{-1}(\vec{r}_a \times \vec{n}_a))} \tag{8c}$$

and $\vec{v}_c$ and $\vec{w}$ are the velocity and angular velocity prior to the collision, respectively, $\vec{n}_a$ is the outward normal vector to the collision point and $\vec{r}_a$ is the relative contact position with respect to the center of mass of the diatomic molecule. Under specular conditions, conservation of energy applied to the modeled degrees of freedom is guaranteed, such that

$$\frac{1}{2}m_{gas}\vec{v}_c^2 + \frac{1}{2}I_1\vec{w}^2 = \frac{1}{2}m_{gas}\vec{v}_r^2 + \frac{1}{2}I_1\vec{w}_r^2. \tag{9}$$

The gas molecule continues on its new trajectory after reemission until it either leaves the domain or impacts the polyatomic structure once more, in which case Eqs. (8a)–(8c) are invoked again.

In the case of diffuse and inelastic reemission, when a gas molecule impinges on the surface of a particle, Eq. (9) does not apply. On the contrary, diffuse and inelastic rules are intended to implicitly consider atomic motion within the ion, and hence to consider complete energy exchange between the modeled degrees of freedom and the ion's internal degrees of freedom, such that all modes of energy are resampled from Maxwell-Boltzmann distributions at the ion temperature. We model diffuse collisions by sampling the reemission angle for the gas molecule from a thermodynamically permissible angular distribution. As described previously,[8,9] Θ, the elevation angle, and Φ, azimuthal angle of reemission, are sampled from the equations:

$$\cos(\Theta) = R_5^{1/2}, \tag{10a}$$

$$\Phi = 2\pi R_6, \tag{10b}$$

where R_5 and R_6 is are uniformly distributed random variables on the interval 0 to 1. We further postulate that the exchange of energy takes place immediately before the impulse (change of momentum), such that the only required change for diffuse and inelastic collisions is to replace $\vec{v}_c$ in Eqs. (8a)–(8c) with the appropriate remission velocity.[8,9] We remark that the choice of replacing $\vec{v}_c$ before the collision is somewhat arbitrary, and alternative means of modeling diffuse collisions could be developed, as could intermediate models between the specular and diffuse limits.

RESULTS AND DISCUSSION

All results reported were obtained by simulating $>10^5$ gas molecule trajectories, using either spherical or cuboid control volumes, with the control volume chosen automatically, as is described previously.[5,8,9] Such conditions led to an accuracy better than 2% for all calculated CCSs.[8]

Single spheres

As a first case study, it is of utility to examine how the implementation of diatomic gas molecules in calculations influences the resulting CCSs of perfectly smooth, singly charged spheres of varying sizes. These calculations enable examination of the relative "scale" at which the ion is modeled; instances wherein the size of the sphere is similar to the gas molecule are akin to all-atom ion models, while instances where the sphere is larger than the gas molecule are encountered in "coarse-grained" ion models, which are often

invoked in examining multiprotein complexes.[14,38] In all circumstances we utilize 4 different types of calculations:

Case 1: Specular collisions in the absence of the long range ion-induced dipole potential.
Case 2: Diffuse collisions in the absence of the long range ion-induced dipole potential.
Case 3: Specular collisions including the long range ion-induced dipole potential (∞–4 potential) at 298 K, with the polarizability of N_2 equivalent to 1.7×10^{-30} m^3.
Case 4: Diffuse collisions including the long range ion-induced dipole potential at 298 K.

For each of these four cases, we perform calculations using a diatomic gas molecule (*model D*) with the aforementioned properties, as well as a monoatomic gas molecule (*model M*) with an equivalent orientationally averaged projected area to the diatomic model (leading to a diameter of 3.1 Å). When *model M* is applied to a perfect sphere, *case* 1 calculations lead to a collision cross section exactly equal to projected area of a sphere with a diameter equal to the sum of the gas and ion diameters, while *case* 2 calculations lead to a collision cross section equal to the *case* 1 collision cross section multiplied by a factor of $1 + \pi/8$ (which are in better agreement with CCSs measured for highly spherical ions).[23,29] The incorporation of diatomic gas molecule structure into CCS calculation complicates this picture further, as does the inclusion of the ion induced dipole potential. Figure 3(a) is a plot the ratios of the CCSs determined with *model D* to those determined with *model M* for all cases, as functions of the ratio of the sphere diameter to the monoatomic model diameter, while Figure 3(b) is a plot of CCSs of all cases and all models normalized by the projected area of the sphere-gas molecule combination. Combined, these two figures show that in the absence of the ion induced dipole potential, with both the specular collision model (*case* 1) and diffuse collision model (*case* 2), the ratio of the CCS from *model D* to the CCS from *model M* is only weakly dependent on the ion to gas molecule size ratio. However, *case* 1 and *case* 2 calculations differ in the manner in which the CCS changes; the use of a diatomic gas molecule model leads to a reduction in CCS for specular collisions (by ~8% for small ions and ~6% for the largest ions examined), but leads to a slight increase in the CCS for diffuse collisions (~4% for small ions and ~1% for the largest ions examined). The use of diatomic gas molecules hence leads to even further disagreement between the specular and diffuse models of collision, for all examined ion to gas molecule size ratios the two models differ in absolute CCS by more than 50% and up to 58% (while they differed by a factor of $\pi/8$, i.e., 39% for monoatomic gas molecules). With the inclusion of the ion-induced dipole potential, at larger ion sizes, *model D* again leads to a reduction in the CCS with specular scattering and an increase in the CCS with diffuse scattering. These results are expected to be similar to the hard-sphere potential results; collisions between gas molecules and sufficiently large ions (for a given charge state) are largely unaffected by long range potentials. However, with both scattering models, as the ion size decreases, inclusion of the ion induced dipole potential leads to clear differences from the hard sphere model, and depending upon the precise value of the ion diameter to the gas molecule diameter, the *model D* collision cross section may be greater than or less than the *model M* CCS.

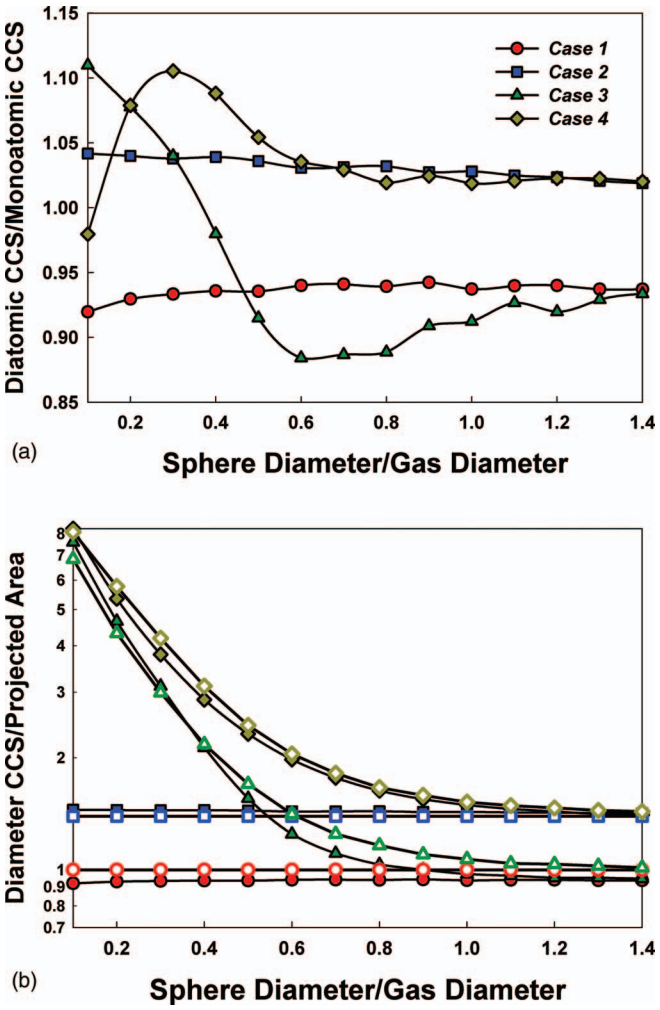

FIG. 3. (a) Ratio of the diatomic gas molecule collision cross section to a spherical gas molecule collision cross section as a function of the ion diameter to gas diameter ratio. The four cases examined are defined in the main text. (b) Ratio of the calculated collision cross section to combined gas molecule-ion projected area section as a function of the ion diameter to gas diameter ratio. Closed symbols – *model D* and open symbols – *model M*.

In total, calculations for spherical ions reveal that the model of the gas molecule applied, the collision rules prescribed for the non-modeled degrees of freedom in ions and gas molecules, as well as the ion-induced dipole potential (for sufficiently small ions) can each influence CCSs. By not recovering a *model D* to *model M* CCS ratio for *case* 1 of $1 + \pi/8$, results also show that the use of specular collision rules with diatomic gas molecules does not lead to agreement with diffuse model calculations (which, to reiterate, do agree with a number of experimental measurements[9,23]); therefore simply modeling the gas molecule as a diatomic structure which collides specularly and elastically will not lead to agreement between measured and calculated CCSs in diatomic gases.

Polyatomic ions

We further examine the influence of modeling gas molecules as rotating diatomic structures for polyatomic

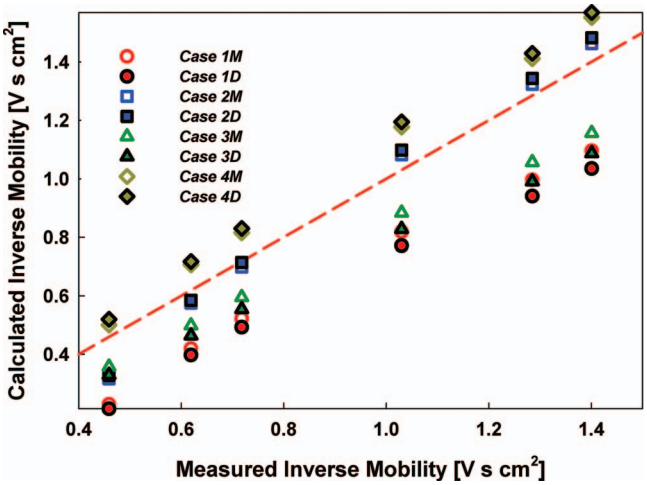

FIG. 4. Predicted inverse mobilities for tetraalkylammonium ions as a function of experimentally measured inverse mobilities for the following ions at 293 K and atmospheric pressure: TMA, TPA, TBA, THA, TDA, and TDDA. The dashed lines denotes 1:1 agreement.

ions, namely singly charged tetra-alkylammonium ions and multiply charged polyethylene glycol (PEG) ions. These ions are selected for examination because not only they have been well characterized by IMS-MS measurements,[31,32,39–42] but also they are either sufficiently small to generate candidate structures in the gas phase (tetraalkylammonium ions)[9] or have clear, charge dependent structures in the gas phase (PEG ions).[32,40] We note this is in contrast to often studied protein and multiprotein complex ions, which do not necessarily have structures resembling their crystal structures or those observed in solution upon introduction in the gas phase;[43–49] the examination of protein ions brings an extra degree of ambiguity into comparison between different collision-reemission models and measurements. Figure 4 displays a comparison of the measured[31] inverse mobilities in air at atmospheric pressure at 293 K for tetramethylammonium$^+$ (TMA^+), tetrapropylammonium$^+$ (TPA^+), tetrabutylammonium$^+$ (TBA^+), tetraheptylammonium$^+$ (THA^+), tetradecylammonium$^+$ (TDA^+), and tetradodecylammonium$^+$ ($TDDA^+$) ions to model predictions for all 4 cases and with both *model D* and *model M* gas molecules. The atomic radii for all atoms in ions are the same as those used in our previous calculations with spherical gas molecules only, and reported results are the average inverse mobilities based on 3-20 conformers for each ion (3 for TMA^+, 6 for TPA^+, 8 for TBA^+, 20 for THA^+, 20 for TDA^+, and 20 for $TDDA^+$), obtained via MM2 molecular dynamic calculations with subsequent linear structure reduction.[9] In our prior report, we found that an empirical diffuse and inelastic reemission rule for spherical gas molecules gave rise to excellent agreement between measured and calculated inverse mobilities when the ion-induced dipole potential was considered (similar to *case* 4, though with a reduced reemission speed). While we again find that diffuse and inelastic reemission rules lead to better agreement between experiments and measurements with diatomic gas molecules, *case* 4 calculations with *model D* were 1.8% greater on average than *model M* and in weaker agreement with experimental results (on average 11.9% larger than the experimental values). The observed difference between *case* 4 *model D* and *case* 4 *model M* calculations is lowest for the largest ion (1.0% for $TDDA^+$) and is 4.0% for the smallest ion (TMA^+). Although the differences between the two gas molecule models are extremely small when compared to the influence of scattering model, like calculations for spherical ions, these results reveal that the gas molecule structure model and the collision-reemission rule model used in CCS calculations are linked; their influences cannot be decoupled from another.

Further evidence of the gas molecule structure-collision rule link is displayed in Figure 5, which presents a comparison of calculations for five +4 PEG ions (PEG-254 (A), PEG-144 (B), PEG-115 (C), PEG-90 (D), and PEG-70 (E)) that

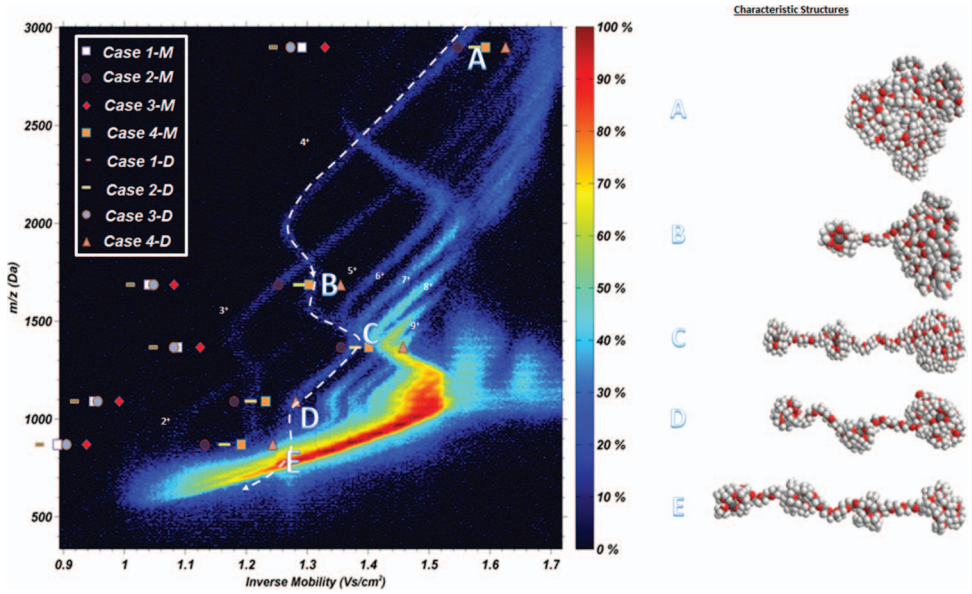

FIG. 5. An experimental mass-mobility contour plot for multiply charged polyethylene glycol ions. For five examined +4 ions (labeled A–E at different points on the dashed line and with characteristic structures shown to the right), mobility calculations are performed, and the resulting predicted m/z and inverse mobility for different model predictions are overlaid on the contour plot.

each have distinct gas phase structures near 300 K. Specifically displayed in Figure 5 are depictions of these structures (determined as described previously)[9] as well as a contour plot of signal intensity as a function of both mass-to-charge (m/z) ratio and inverse mobility, which was measured in atmospheric pressure air near 300 K by Larriba and Fernandez de la Mora[32] for electrospray generated PEG ions using differential mobility analysis-time-of-flight mass spectrometry. As described in their work, ions of a specific charge state are grouped into specific bands in contour plots such as that in Figure 5, and within these bands structural transitions for ions are marked by clear changes in the bands' slopes (i.e., the change in mass-to-charge ratio per unit change in inverse mobility). The dashed white line highlights the +4 band, and the letters label specific PEG ions examined here. Also overlaid on the contour plot are the inverse mobilities calculated for each structure using the 4 noted collision rule cases and two different gas molecules (note all results for a specific ion appear at the same mass-to-charge ratio, as this is known). Calculations are again grouped primarily by the collision rules (specular-elastic versus diffuse-inelastic) which are invoked, with the ion induced dipole minimally influencing calculations (except for the smallest PEG ions). As is observed for spherical ions, diatomic gas calculations typically lead to lower CCSs (higher mobilities) than monoatomic gas molecule calculations by ∼4% with specular-elastic collision rules, while with diffuse-inelastic collision rules they lead to slightly larger CCSs. While these differences are small, these results call into question the possibility with current approaches of distinguishing closely related ion structures from one another by ion mobility measurements. Current IMS instrumentation enables separation of ions which differ from one another in CCS by less than 2%, yet because the impingement reemission rules to invoke in calculations are not known (and need to be modified based on the modeled gas molecule structure) and can alter results by more than 2%, clear identification of a particular isomer by IMS alone may prove difficult in most gases (Table I).

Discussion of current status of CCS calculation approaches

As a final note, we remark on differences between the calculation approach applied in this work and those invoked elsewhere. As noted above, the IMoS gas molecule scattering algorithms allow for inference of the orientationally averaged collision cross section from direct quantification of the rate of momentum transfer (i.e., the drag force) from gas molecules to an ion, for a small (relative to the mean thermal speed) bulk velocity difference between the gas and ion. As inputs, calculations require a specific ion and gas molecule structural model (including atomic radii), the potential interactions to be considered, and finally, prescribed impingement-reemission rules.[8,9] With hard sphere interactions, specular-elastic impingement-reemission, and spherical gas molecules, IMoS calculations give rise to similar results to the standard EHSS algorithm from MOBCAL,[11,15] with the exception of highly skewed (i.e., high aspect ratio) ions, for which IMoS and MOBCAL perform orientational averaging in different manners. Similarly, with Lennard-Jones potentials, monatomic gas molecules, and specular-elastic scattering, IMoS calculations agree well with the TM method calculations of MOBCAL,[10] and we find that both approaches have similar computational cost. While IMoS calculations presently make use of spheres as the base units for ion and gas molecule structures, as has been demonstrated for MOBCAL calculations by Shvartsburg and co-workers using electron density isosurfaces,[13,19] with some modification to the algorithms IMOS calculations could also be performed using more sophisticated models of ions and gas molecules.

What has been distinct between IMoS calculations and MOBCAL calculations is the manner in which CCS calculations have been modified for diatomic gases. As discussed here, we find evidence for non-specular, inelastic scattering of gas molecules (when rigid ion and gas molecules are considered, even if the gas molecule modeled as a rotating diatom), and we suggest that in many instances hard-sphere models may still be used for CCS calculations in N_2, with diffuse-inelastic impingement-reemission rules. Meanwhile, in modifying MOBCAL calculations, Kim and co-workers[12,22,50] have continued to use specular-elastic impingement-reemission rules and instead fit the Lennard-Jones parameters between gas molecules and ions to find agreement between calculations and measurements. These two approaches are the converse of one another; for given hard-sphere interactions we have modified the impingement-reemission rules (the kinetic energy exchange) to find agreement between measurements and calculations while researchers using MOBCAL have, for a preset impingement-reemission rule, fit the ion-gas molecule potential energy (which hence requires use of a trajectory method, TM, calculation, and greater computational cost). For a given temperature, gas molecule, and ion, fitting either the impingement-reemission rule (with fixed short range potentials) or the potential interactions (with fixed impingement-reemission rules) appears to facilitate agreement between calculations

TABLE I. Calculated CCS for the PEG ions depicted in Figure 5 in A^2.

PEG ion number	Case 1, model M	Case 1, model D	Case 2, model M	Case 2, model D	Case 3, model M	Case 3, model D	Case 4, model M	Case 4, model D	Experimental
70	784	752.2	995.7	1024.3	765.1	796.7	1048.6	1093.9	1091
90	836.1	802.4	1038.3	1062	816.4	754.1	1083.7	1127.1	1123.2
115	956.9	915.8	1191.8	1212.6	941.2	951.3	1232.3	1281.6	1225.1
144	915.1	883.1	1102	1131.8	890.9	922.3	1146.1	1191.6	1151.7
254	1135.8	1088.7	1360.3	1384.6	1103.6	1119.3	1400.2	1429.4	1365.9

and measurements. As shown, here, however, the ion structure, gas molecule structure, collision rules, and potentials invoked are all coupled to one another, and to remove the need to "fit" any of these parameters in model calculations, further examination of the physics governing ion-gas molecule collisions under conditions relevant to IMS measurement is necessary.

We also distinguish between algorithms in which an attempt is made to model gas molecule-ion collisions and extract CCS information from collision modeling (namely, the IMoS methods and MOBCAL methods), and approaches in which *ad hoc* approximations are made to determine CCSs. Specifically, the recently developed projected superposition approximation (PSA) method,[51] in which the CCS is calculated as the product of an effective projected area for an ion-gas molecule combination and a "shape factor," is an approach which appears to be originally developed as a computationally efficient manner to determine CCSs in agreement with MOBCAL's TM calculations. While in IMoS and MOBCAL calculations the fitting parameters involved link to the physics of gas molecule-ion interactions and collisions, in the PSA method, the approach itself is by definition unphysical (i.e., gas molecule impingement-reemission is not modeled, and rigorously the CCS is not proportional to the product of a projected area and a shape factor under all circumstances). To our knowledge, no attempt to account for diffuse/inelastic gas molecule impingement-reemission has been made with the PSA method, though it may be possible to find PSA method inputs which lead to CCSs in agreement with diffuse-inelastic scattering calculations.

CONCLUSIONS

Diatomic gas molecule structures and the rotational energy of gas molecules have been incorporated into CCS calculations in a computationally efficient manner. In large part, calculations show that the influence of diatomic gas molecules on calculations is dependent on the gas molecule size to sizes of the entities comprising the ion (atoms in most models). Further, calculations reveal that the effects of ion structure, gas molecule structure, collision rules, and the large range potential are linked, and as more rigorous calculation methods for CCSs are developed, all of these effects must be considered together. Further, while short-range, Lennard-Jones potentials were not considered in the calculations reported here, we note that their inclusion would not alter the conclusions of this work. Finally, in instances where ions are modeled as spheres (as is commonplace in the study of aerosols), it has been customary to explain experimentally observed CCSs[28,52,53] by invoking an accommodation coefficient, a fraction of collisions which are diffuse and inelastic (with the remaining specular). Most data for large (>10 nm) ions and a number of number of smaller, reasonable spherical ions[23,24] lead to a value of $\sim$0.91 for the accommodation coefficient. However, this value is based upon an assumed spherical gas molecule. The accommodation coefficient would need to be decreased for a diatomic gas molecule, demonstrating that it too is simply a "fit" parameter to explain experimental results.

ACKNOWLEDGMENTS

This work was supported by National Science Foundation grant NSF-CHE-1011810. C.L.-A. also acknowledges support from a Ramon Areces Fellowship.

[1] J. Fernandez de la Mora, L. de Juan, T. Eichler, and J. Rosell, TrAC, Trends Anal. Chem. **17**, 328 (1998).
[2] G. von Helden, M. T. Hsu, P. R. Kemper, and M. T. Bowers, J. Chem. Phys. **95**, 3835 (1991).
[3] E. W. McDaniel and E. A. Mason, *The Mobility and Diffusion of Ions in Gases* (Wiley, 1973).
[4] A. A. Shvartsburg, S. V. Mashkevich, and K. W. M. Siu, J. Phys. Chem. A **104**, 9448 (2000).
[5] H. Ouyang, C. Larriba-Andaluz, D. R. Oberreit, and C. J. Hogan, J. Am. Soc. Mass Spectrom. **24**, 1833 (2013).
[6] Z. Li and H. Wang, Phys. Rev. E **68**, 061206 (2003).
[7] T. Wyttenbach, C. Bleiholder, and M. T. Bowers, Anal. Chem. **85**, 2191 (2013).
[8] C. Larriba and C. J. Hogan, J. Comput. Phys. **251**, 344 (2013).
[9] C. Larriba and C. J. Hogan, J. Phys. Chem. A **117**, 3887 (2013).
[10] M. F. Mesleh, J. M. Hunter, A. A. Shvartsburg, G. C. Schatz, and M. F. Jarrold, J. Phys. Chem. **100**, 16082 (1996).
[11] A. A. Shvartsburg and M. F. Jarrold, Chem. Phys. Lett. **261**, 86 (1996).
[12] H. I. Kim *et al.*, Anal. Chem. **81**, 8289 (2009).
[13] Y. Alexeev, D. G. Fedorov, and A. A. Shvartsburg, J. Phys. Chem. A **118**, 6763 (2014).
[14] B. T. Ruotolo, J. L. P. Benesch, A. M. Sandercock, S. J. Hyung, and C. V. Robinson, Nat. Protoc. **3**, 1139 (2008).
[15] A. A. Shvartsburg, S. V. Mashkevich, E. S. Baker, and R. D. Smith, J. Phys. Chem. A **111**, 2002 (2007).
[16] D. W. Mackowski, J. Aerosol Sci. **37**, 242 (2006).
[17] A. A. Shvartsburg, B. Liu, K. W. M. Siu, and K. M. Ho, J. Phys. Chem. A **104**, 6152 (2000).
[18] B. S. Kinnear, D. T. Kaleta, M. Kohtani, R. R. Hudgins, and M. F. Jarrold, J. Am. Chem. Soc. **122**, 9243 (2000).
[19] A. A. Shvartsburg, B. Liu, M. F. Jarrold, and K. M. Ho, J. Chem. Phys. **112**, 4517 (2000).
[20] R. R. Hudgins, M. Imai, M. F. Jarrold, and P. Dugourd, J. Chem. Phys. **111**, 7865 (1999).
[21] P. Dugourd, R. R. Hudgins, and M. F. Jarrold, Chem. Phys. Lett. **267**, 186 (1997).
[22] I. Campuzano *et al.*, Anal. Chem. **84**, 1026 (2012).
[23] C. Larriba, C. J. Hogan, M. Attoui, R. Borrajo, J. Fernandez-Garcia, and J. Fernandez de la Mora, Aerosol Sci. Technol. **45**, 453 (2011).
[24] B. K. Ku and J. Fernandez de la Mora, Aerosol Sci. Technol. **43**, 241 (2009).
[25] I. V. Adamovich and J. W. Rich, J. Chem. Phys. **109**, 7711 (1998).
[26] H. Ambaye and J. R. Manson, Phys. Rev. E **73**, 031202 (2006).
[27] H. Ambaye and J. R. Manson, J. Chem. Phys. **125**, 084717 (2006).
[28] R. A. Millikan, Phys. Rev. **22**, 1 (1923).
[29] P. S. Epstein, Phys. Rev. **23**, 710 (1924).
[30] Z. G. Li and H. Wang, Phys. Rev. Lett. **95**, 014502 (2005).
[31] S. Ude and J. Fernandez de la Mora, J. Aerosol Sci. **36**, 1224 (2005).
[32] C. Larriba and J. Fernandez de la Mora, J. Phys. Chem. B **116**, 593 (2012).
[33] M. Niwa, K. Yamazaki, and Y. Murakami, Ind. Eng. Chem. Res. **30**, 38 (1991).
[34] E. C. Kemble, Phys. Rev. **8**, 689 (1916).
[35] See supplementary material at http://dx.doi.org/10.1063/1.4901890 for a description of the application of Rotation Matrices.
[36] Y. Wang and M. T. Mason, Proc. Int. Conf. Rob. Autom. **4**, 678 (1987).
[37] D. Baraff, IEEE Comput. Graphics Appl. **15**, 63 (1975).
[38] T. L. Pukala *et al.*, Structure **17**, 1235 (2009).
[39] S. Ude, J. Fernandez de la Mora, and B. A. Thomson, J. Am. Chem. Soc. **126**, 12184 (2004).
[40] C. Larriba, J. Fernandez de la Mora, and D. E. Clemmer, J. Am. Soc. Mass Spectrom. **25**, 1332 (2014).
[41] E. Criado-Hidalgo, J. Fernández-García, and J. Fernández de la Mora, Anal. Chem. **85**, 2710 (2013).
[42] S. Trimpin and D. E. Clemmer, Anal. Chem. **80**, 9073 (2008).
[43] F. W. McLafferty, S. Castro, and K. Breuker, Eur. J. Mass Spectrom. **16**, 437 (2010).

[44]M. Schennach and K. Breuker, Angew. Chem., Int. Ed. **53**, 164 (2014).
[45]O. S. Skinner, F. W. McLafferty, and K. Breuker, J. Am. Soc. Mass Spectrom. **23**, 1011 (2012).
[46]C. J. Hogan, B. T. Ruotolo, C. V. Robinson, and J. Fernandez de la Mora, J. Phys. Chem. B **115**, 3614 (2011).
[47]J. Freeke, M. F. Bush, C. V. Robinson, and B. T. Ruotolo, Chem. Phys. Lett. **524**, 1 (2012).
[48]L. J. Han, S. J. Hyung, and B. T. Ruotolo, Angew. Chem., Int. Ed. **51**, 5692 (2012).
[49]A. Maiber, V. Premnath, A. Ghosh, T. A. Nguyen, M. Attoui, and C. J. Hogan, Phys. Chem. Chem. Phys. **13**, 21630 (2011).
[50]H. Jung, K. Han, G. W. Mulholland, D. Y. H. Pui, and J. H. Kim, J. Aerosol Sci. **65**, 42 (2013).
[51]C. Bleiholder, T. Wyttenbach, and M. T. Bowers, Int. J. Mass Spectrom. **308**, 1 (2011).
[52]M. D. Allen and O. G. Raabe, Aerosol Sci. Technol. **4**, 269 (1985).
[53]J. H. Kim, G. W. Mulholland, S. R. Kukuck, and D. Y. H. Pui, J. Res. Natl. Inst Stand. Technol. **110**, 31 (2005).